Perovskites Hot Paper

How to cite: *Angew. Chem. Int. Ed.* **2022,** *61,* e202115875
International Edition: doi.org/10.1002/anie.202115875
German Edition: doi.org/10.1002/ange.202115875

Interfacial Chemistry Triggers Ultrafast Radiative Recombination in Metal Halide Perovskites

Haiyun Dong[+], Chunhuan Zhang[+], Weijie Nie, Shengkai Duan, Christian N. Saggau, Min Tang, Minshen Zhu, Yong Sheng Zhao, Libo Ma,* and Oliver G. Schmidt**

Abstract: Efficient radiative recombination is essential for perovskite luminescence, but the intrinsic radiative recombination rate as a basic material property is challenging to tailor. Here we report an interfacial chemistry strategy to dramatically increase the radiative recombination rate of perovskites. By coating aluminum oxide on the lead halide perovskite, lead–oxygen bonds are formed at the perovskite-oxide interface, producing the perovskite surface states with a large exciton binding energy and a high localized density of electronic state. The oxide-bonded perovskite exhibits a ≈500 fold enhanced photoluminescence with a ≈10 fold reduced lifetime, indicating an unprecedented ≈5000 fold increase in the radiative recombination rate. The enormously enhanced radiative recombination promises to significantly promote the perovskite optoelectronic performance.

[*] Dr. H. Dong,[+] Dr. W. Nie, S. Duan, C. N. Saggau, Dr. M. Tang, Dr. M. Zhu, Dr. L. Ma, Prof. O. G. Schmidt
Institute for Integrative Nanosciences, Leibniz IFW Dresden, 01069 Dresden (Germany)
E-mail: l.ma@ifw-dresden.de
oliver.schmidt@main.tu-chemnitz.de

Dr. C. Zhang,[+] Prof. Y. S. Zhao
Key Laboratory of Photochemistry, Institute of Chemistry, Chinese Academy of Sciences, 100190 Beijing (China)
E-mail: yszhao@iccas.ac.cn

S. Duan, C. N. Saggau, Prof. O. G. Schmidt
Material Systems for Nanoelectronics, TU Chemnitz, 09107 Chemnitz (Germany)
and
Research Center for Materials, Architectures and Integration of Nanomembranes, TU Chemnitz, 09126 Chemnitz (Germany)

Prof. Y. S. Zhao
School of Chemical Sciences, University of Chinese Academy of Sciences, 100049 Beijing (China)

Prof. O. G. Schmidt
Nanophysics, Faculty of Physics, TU Dresden, 01062 Dresden (Germany)

[+] These authors contributed equally to this work.

Introduction

Metal halide perovskites are extremely attractive for optoelectronic and photonic applications, such as solar cells, photodetectors, light-emitting diodes, and lasers, because they combine solution-processability with remarkable semiconductor characteristics.[1] Since a high radiative efficiency is essential for high-performance optoelectronic devices, considerable research effort has been devoted to enhancing radiative recombination and suppressing non-radiative recombination in the perovskites.[2] The radiative recombination rate can be increased by localizing charge carriers via quantum confinement[3] and ion doping[4] or by increasing the density of photonic state with metamaterials/metasurfaces,[5] while the trap-assisted non-radiative recombination rate can be reduced through recrystallization of perovskites[6] or chemical passivation of defects.[7] The enhancement of intrinsic radiative recombination in perovskite materials represents a more direct and powerful strategy for improving the perovskite optoelectronic performance, especially that of luminescent devices.[8] However, current quantum confinement and ion doping strategies suffer from limited increases (<100 times, Table S1) in radiative recombination rate because of their failure to significantly affect the intrinsic electronic band structure of perovskites.

In this work, we demonstrated an interfacial chemistry strategy of modifying metal halide perovskites to dramatically enhance their radiative recombination rate. By coating aluminum oxide onto the lead halide perovskite film via atomic layer deposition, lead-oxygen bonds are formed at the perovskite-oxide interface, which results in a ≈500 fold enhanced photoluminescence intensity together with a ≈10 fold reduced lifetime, corresponding to an unprecedented ≈5000 fold increase in the radiative recombination rate. Investigations of excited-state dynamics and calculations of electronic band structures reveal that the giant enhancement of radiative recombination is attributed to the formation of oxide-bonded perovskite surface states with a large exciton binding energy and a high localized density of electronic state. As a result, the oxide-coated perovskite film allows for stable and efficient optical gain with a remarkably low threshold. The discovery that a surface chemical modification of perovskites enhances radiative recombination rate provides valuable guidance for perovskite optimization towards improved optoelectronic performance.

Results and Discussion

The films of cesium lead bromide ($CsPbBr_3$) perovskites were fabricated through anti-solvent assisted spin-coating and modified by aluminum oxides (Al_2O_3) via plasma-enhanced atomic layer deposition (PEALD) (Figure 1a, see Supporting Information for further details). The thickness of as-prepared perovskite films is around 125 nm (Figure S1). Scanning electron microscopy (SEM) images (Figure 1b,d) and atomic force microscopy images (Figure S2) show that the $CsPbBr_3$ films have very similar surface morphologies with a surface roughness of ≈27 nm before and after the Al_2O_3 modification. Energy-dispersive X-ray spectroscopy (EDS) images (Figure 1c,e) exhibit uniform distributions of Cs, Pb, and Br with molar ratios of 0.96:1.00:3.03 and 0.94:1.00:3.02 for the $CsPbBr_3$ films without and with the Al_2O_3 coating, respectively, which both conform well to the $CsPbBr_3$ stoichiometry. In addition, the uniform Al and O distributions indicate the formation of a dense Al_2O_3 film on the perovskite film. X-ray diffraction (XRD) patterns show that the bare and Al_2O_3-coated $CsPbBr_3$ films yield the same diffraction peaks that can be indexed to the $CsPbBr_3$ orthorhombic crystal phase (Figure 1f).[6b,9] Overall, the $CsPbBr_3$ perovskite films maintain their original morphologies, components, and crystal structures after the Al_2O_3 modification. These results exclude the potential possibility that the $CsPbBr_3$ perovskite film experiences changes in the morphology, component, or crystal structure during the Al_2O_3 deposition, which might affect the perovskite luminescence.

X-ray photoelectron spectroscopy (XPS) measurements were conducted to probe the interfacial interaction between the $CsPbBr_3$ and Al_2O_3. While the Cs and Br 3*d* peaks show no shift (Figure S3), the Pb 4*f* peaks experience a clear shift towards high binding energy after the Al_2O_3 modification (Figure 1g). In the bare $CsPbBr_3$ film, the two Pb XPS peaks observed at 143.0 and 138.1 eV correspond to Pb $4f_{5/2}$ and Pb $4f_{7/2}$ levels in the Pb–Br octahedra, respectively.[10] After the Al_2O_3 coating, the Pb 4*f* peaks become broad and can be deconvolved into two components: the original doublet peaks of the Pb–Br octahedra and two additional high-binding-energy peaks at 143.5 and 138.6 eV. The two newly emerged peaks can be assigned to the Pb–O bonds at the $CsPbBr_3$-Al_2O_3 interface (Figure 1a).[11] The formation of the Pb–O bonds is expected to significantly alter the electronic band structure of the $CsPbBr_3$ perovskite leading to unique band-edge emission phenomena.

Figure 2a,b show the photoluminescence (PL) images of the $CsPbBr_3$ perovskite films with and without Al_2O_3 modification under ultraviolet (UV) excitation. The UV light power was kept constant, while the UV exposure time for PL imaging of the bare perovskite was 100 times longer than that of the Al_2O_3-coated one. Apparently, the Al_2O_3-coated $CsPbBr_3$ film exhibits a much stronger green light emission. As shown in the corresponding PL spectra (Figure 2c), the PL intensity of the $CsPbBr_3$ film increases

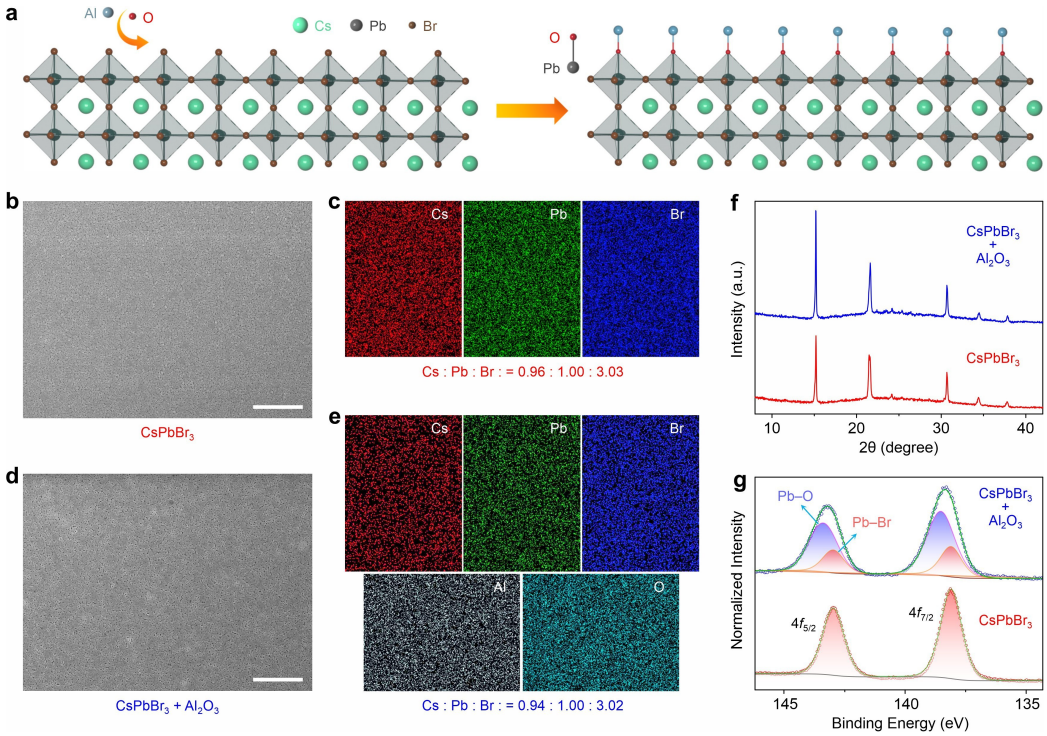

Figure 1. a) Schematic diagram showing the chemical modification of the $CsPbBr_3$ perovskite with Al_2O_3. b) SEM image and c) EDS mapping of a typical $CsPbBr_3$ perovskite film. Scale bar is 10 μm. d) SEM image and e) EDS mapping of a $CsPbBr_3$ perovskite film coated with Al_2O_3 of 40 ALD cycles. Scale bar is 10 μm. f) XRD patterns of the $CsPbBr_3$ perovskite films with and without Al_2O_3 coating, corresponding to the same $CsPbBr_3$ orthorhombic phase. g) XPS spectra of Pb 4*f* of the $CsPbBr_3$ perovskite films with and without Al_2O_3 coating, revealing the formation of Pb–O bonds.

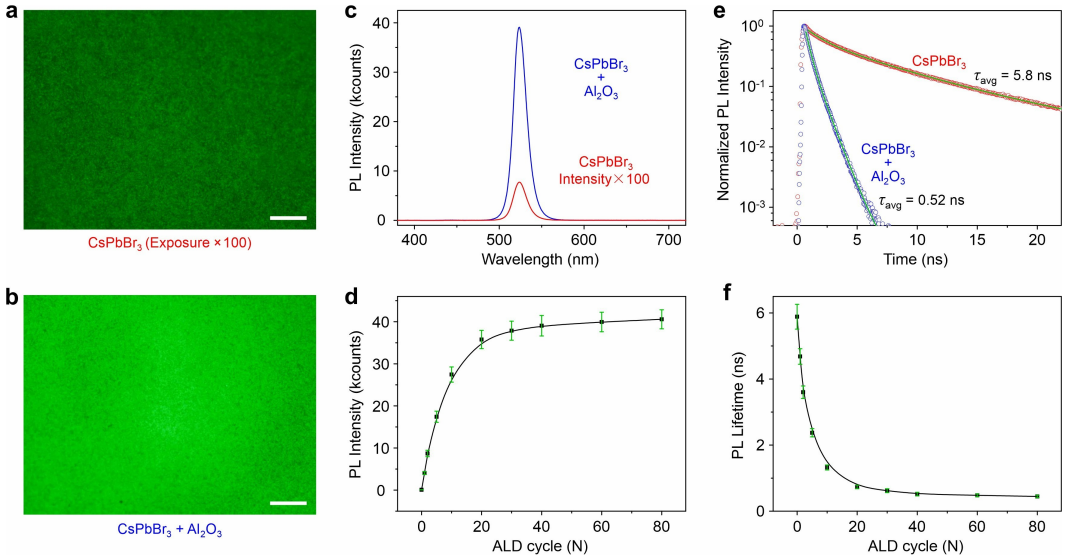

Figure 2. a, b) PL images of bare and Al_2O_3-coated $CsPbBr_3$ perovskite films under UV (330–380 nm) excitation with the same power. The UV exposure time for PL imaging of the bare perovskite is 100 times longer than that of the Al_2O_3-coated one. Scale bars are 20 μm. c) PL spectra of the $CsPbBr_3$ perovskite films with and without Al_2O_3 coating under same UV excitations, showing a ≈500 fold PL enhancement after Al_2O_3 coating. d) PL intensities of the $CsPbBr_3$ perovskite films coated by Al_2O_3 with different ALD cycles. e) PL decay profiles and fitted curves of the $CsPbBr_3$ perovskite films with and without Al_2O_3 coating under the same excitation powers. f) PL lifetimes of the $CsPbBr_3$ perovskite films as a function of Al_2O_3 ALD cycles.

≈500 times after Al_2O_3 modification. Accordingly, the PL quantum yield of the $CsPbBr_3$ perovskite film increases from ≤0.1 % (instrument limited) to 8.6 %. A systematic study was further carried out on the PL of the $CsPbBr_3$ films coated by Al_2O_3 with an increasing number of ALD cycles (Figure S4). The PL intensity of the $CsPbBr_3$ film strongly increases up to 20 ALD cycles and then levels off with additional ALD cycles (Figure 2d). This indicates that the formation of a dense Al_2O_3 film on the whole surface of a $CsPbBr_3$ film requires at least 20 ALD cycles.

Figure 2e shows the PL decay profiles of the bare and Al_2O_3-coated $CsPbBr_3$ films under the same excitation powers, which both can be well fitted exponentially with average PL lifetimes of 5.8 and 0.52 ns, respectively. We systematically investigated the PL decay dynamics of the $CsPbBr_3$ films coated by Al_2O_3 with different ALD cycles (Figure S5). When the ALD cycle increases, the PL lifetime of the $CsPbBr_3$ film first declines rapidly and then approaches a plateau value (Figure 2f). When more than 20 ALD cycles are employed, the PL lifetime is reduced more than 10 times. Apparently, the decrease of the PL lifetime corresponds well to the increase of the PL intensity (Figure 2d, f), which indicates that the PL enhancement in the Al_2O_3-modified $CsPbBr_3$ perovskite is mainly caused by a more efficient radiative recombination. The radiative recombination rate can be evaluated by the ratio of PL quantum yield to PL lifetime.[8] Because the light absorption coefficient of the $CsPbBr_3$ film remains nearly unchanged before and after Al_2O_3 modification (Figure S6), the PL intensity is in direct proportion with the PL quantum yield. Hence, the ≈10 fold PL lifetime reduction, together with the ≈500 fold PL intensity enhancement, reveals a ≈5000 fold increase in the radiative recombination rate of perovskite, which is much larger than those reported by other strategies (Table S1).

One of the most intriguing features of the perovskites is their chemically tailorable band gaps supporting tunable light emission.[12] Here, we fabricated the $CsPbClBr_2$ and $CsPbBr_{1.5}I_{1.5}$ perovskite films with cyan and red emission, respectively, and modified them with Al_2O_3 (Figure S7). Both of the $CsPbClBr_2$ and $CsPbBr_{1.5}I_{1.5}$ films exhibit increased PL intensities and reduced PL lifetimes after the Al_2O_3 modification, corresponding to the remarkable enhancement of radiative recombination. This indicates that the interfacial chemistry strategy of enhancing radiative recombination is universal for the perovskites with different halogen compositions.

To reveal the mechanism underlying the radiative recombination enhancement, we first investigated the excited-state dynamics in the $CsPbBr_3$ perovskites. The PL spectra of bare and Al_2O_3-coated $CsPbBr_3$ perovskite films were recorded at different temperatures ranging from 5 to 300 K (Figure 3a,b). With the decrease of temperature, the light emissions from both the bare and Al_2O_3-coated $CsPbBr_3$ films undergo notable red shifts, spectral narrowing, and intensity increases (Figure 3c–e). The temperature (T) dependent PL peak energy (E), full width at half maximum (FWHM, Γ), and integrated intensity (I) satisfy the following Equations (1)–(3), respectively:[13]

$$E = E_0 + A_{TE}T + A_{EP}\left(\frac{2}{\exp\left(\frac{E_{AP}}{k_B T} - 1\right)} + 1\right) \quad (1)$$

where A_{TE} and A_{EP} are the contribution coefficients of lattice thermal expansion and electron-phonon interaction

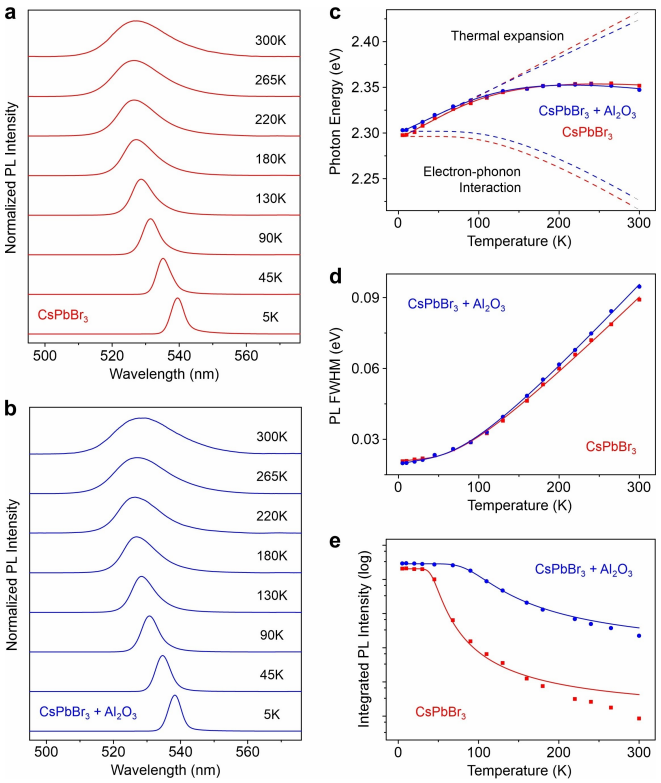

Figure 3. a, b) PL spectra of bare and Al_2O_3-coated $CsPbBr_3$ perovskite films measured at different temperatures. c–e) Temperature-dependent PL peak energies, PL FWHMs and integrated PL intensities of the $CsPbBr_3$ perovskite films with and without Al_2O_3 coating.

to the band gap variation, respectively, E_{AP} is the average phonon energy, and k_B is the Boltzmann constant;

$$\Gamma = \Gamma_0 + \gamma_A T + \frac{\gamma_{LO}}{\exp\left(\frac{E_{LO}}{k_B T}\right) - 1} \quad (2)$$

where γ_A and γ_{LO} are the contribution coefficients of exciton-acoustic phonon and exciton-longitudinal optical phonon interactions to the FWHM variation, respectively, and E_{LO} is the longitudinal optical phonon energy;

$$I = \frac{I_0}{1 + A\exp(-E_b/k_B T)} \quad (3)$$

where A is a pre-exponential factor and E_b is the exciton binding energy.

Table 1 lists the fitting results of the contribution coefficients of the lattice expansion to band gap variation, phonon energies, and exciton binding energies. The band gap of Al_2O_3-coated $CsPbBr_3$ experiences less influence from the lattice expansion than that of bare $CsPbBr_3$, indicating a $CsPbBr_3$ lattice anchoring by the surface Al_2O_3 with a smaller thermal expansion coefficient.[14] Meanwhile, the Al_2O_3-coated $CsPbBr_3$ exhibits larger phonon energies than the bare $CsPbBr_3$, which is attributed to the formation of interfacial PbO and Al_2O_3 with higher rigidities.[15] These results demonstrate that the highly efficient light emission in the Al_2O_3-coated $CsPbBr_3$ perovskite film originates from the $CsPbBr_3$ surface states chemically bonded with Al_2O_3. Besides, the Al_2O_3-modified $CsPbBr_3$ surface states have a larger exciton binding energy than the bare $CsPbBr_3$ because the interfacial PbO and Al_2O_3 with lower dielectric constants weakens the Coulomb screening of electron-hole pairs.[16] The large exciton binding energy induces a large electron-hole capture rate and a high radiative transition probability, accounting for the ultrafast radiative recombination in the Al_2O_3-coated $CsPbBr_3$ perovskite film.

The $CsPbBr_3$ surface radiative states were further investigated through the excitation power dependent excited-state dynamics. We collected the PL spectra of bare and Al_2O_3-coated $CsPbBr_3$ perovskite films under different excitation powers ranging from 18.7 nW to 16.8 μW (Figure 4a, b). The excitation power (P) dependent integrated PL intensity (I) follows an exponential function, $I \propto P^k$,

Table 1: Fitting results of lattice expansion contributions to band gap variation, phonon energies, and exciton binding energies.

	A_{TE} [meV K^{-1}]	E_{AP} [meV]	E_{LO} [meV]	E_b [meV]
$CsPbBr_3$	0.46	36.6	21.0	37.2
$CsPbBr_3 + Al_2O_3$	0.41	40.1	23.4	52.8

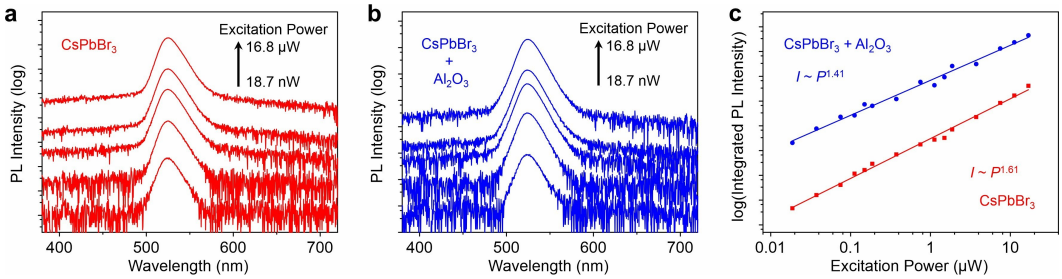

Figure 4. a, b) PL spectra of bare and Al_2O_3-coated $CsPbBr_3$ perovskite films under different excitation powers. c) Integrated PL intensities of the $CsPbBr_3$ perovskite films with and without Al_2O_3 coating versus excitation powers.

where the power coefficient $k=1$ and 2 denotes monomolecular and bimolecular recombination processes, respectively.[17] The fitted power k values fall between 1 and 2 for both bare and Al_2O_3-modified $CsPbBr_3$ (Figure 4c), indicating the coexistence of exciton and free charge carrier recombination processes. The Al_2O_3-modified $CsPbBr_3$ perovskite has a smaller k value, implying a higher proportion of the exciton recombination, which further confirms its larger exciton binding energy.

For a deeper understanding of the ultrafast radiative recombination, we measured the PL characteristics of the $CsPbBr_3$ perovskite films from the substrate side (Figure S8). After the Al_2O_3 coating, the PL intensity increases $\approx$480 times and the PL lifetime decreases $\approx$10 times. Apparently, the ultrafast radiative recombination in the Al_2O_3-modified $CsPbBr_3$ film detected from the substrate side is almost the same as that from the perovskite surface (Figure 2). This phenomenon can be explained by a physical picture for the ultrafast photogenerated carrier dynamics as follows. Optical excitation leads to the generation of carriers in both perovskite bulk and surface phases. The $CsPbBr_3$ bulk phase with a long intrinsic carrier lifetime serves as a carrier reservoir, while the Al_2O_3-modified $CsPbBr_3$ surface state offers an ultrafast radiative recombination pathway for the photogenerated carriers. Because the carrier diffusion length (up to 10 μm) of the $CsPbBr_3$ perovskite is much larger than the $CsPbBr_3$ film thickness ($\approx$125 nm),[18] the photogenerated carriers in the bulk phase diffuse rapidly to the perovskite surface and are captured by the $CsPbBr_3$ surface states with a larger exciton binding energy. As a result, almost all radiative decay of the photogenerated carriers in the Al_2O_3-modified $CsPbBr_3$ perovskite films occur through the surface ultrafast recombination pathway.

To further elucidate the mechanism underlying the giant radiative recombination enhancement, we calculated the electronic band structures of $CsPbBr_3$ perovskites before and after Al_2O_3 chemical modification (Figure 5a, b, see Supporting Information for calculation details).[19] Both the bare and Al_2O_3-modified $CsPbBr_3$ perovskites have direct band gaps at the G-point of the Brillouin zone (Figure 5c, d, left panels), representing a prerequisite for efficient radiative recombination. From the electronic band dispersion, we extracted the effective masses of the electron and hole (m_e and m_h) and further calculated the reduced electron-hole masses (m_r) (Table 2). Compared with the bare $CsPbBr_3$, the Al_2O_3-modified $CsPbBr_3$ perovskite has a larger reduced electron-hole mass, which is in good agreement with its larger exciton binding energy as the Equation (4):[1d]

$$E_b = \frac{m_r e^4}{8\pi h^2 \varepsilon^2} \tag{4}$$

where e is the elementary charge, h is the Planck constant, and ε is the dielectric constant. In addition, the Al_2O_3-modified $CsPbBr_3$ perovskite exhibits higher densities of electronic states in both valence and conduction bands than the bare $CsPbBr_3$ perovskite (Figure 5c, d right panels), providing more transition pathways for the radiative recombination. Furthermore, we calculated the real-space distributions of the densities of electronic states at the conduction band minima of the bare and Al_2O_3-modified $CsPbBr_3$ perovskites (Figure 5e, f). The density of electronic

Table 2: Calculated effective masses and reduced masses of the electron and hole.

	m_e	m_h	m_r
$CsPbBr_3$	1.25	0.26	0.21
$CsPbBr_3+Al_2O_3$	1.13	0.42	0.31

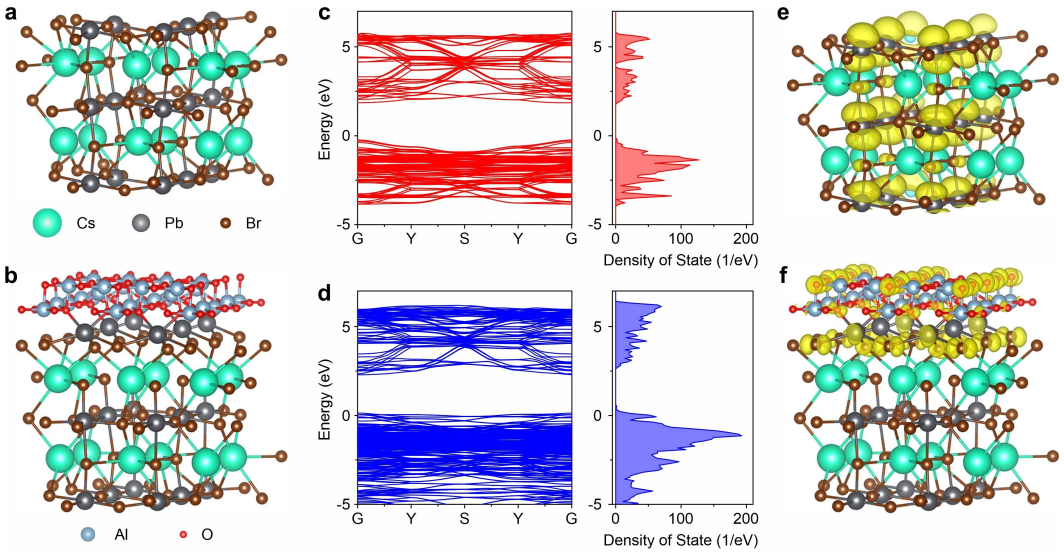

Figure 5. a, b) Theoretical models of orthorhombic-phase $CsPbBr_3$ perovskites without and with Al_2O_3 chemical modification. c, d) Calculated electronic band structures and projected densities of electronic states of the $CsPbBr_3$ perovskites without and with Al_2O_3 modification. e, f) Real-space distributions of the densities of electronic states at conduction band minima of the bare and Al_2O_3-modified $CsPbBr_3$ perovskites.

states uniformly distributes in the $CsPbBr_3$ lattice before the Al_2O_3 coating, but becomes localized at the $CsPbBr_3$-Al_2O_3 interface after the Al_2O_3 modification. The localization corresponds to an increase in the electron-hole wave function overlap in the Al_2O_3-modified $CsPbBr_3$ perovskite, which significantly enhances the radiative recombination probability.[4c,8] Overall, both the increase and localization of the density of electronic states contribute to strongly enhancing the radiative recombination rate in the Al_2O_3-modified $CsPbBr_3$ perovskite.

To sum up, by probing the excited-state dynamics and electronic band structures, we reveal that the giant enhancement of the radiative recombination is attributed to the formation of oxide-bonded perovskite surface states with a large exciton binding energy and a high localized density of electronic states. The enhanced radiative recombination promises to improve the perovskite optoelectronic performance, especially in luminescence applications. For example, the optical gain increases with the radiative recombination rate as the stimulated emission cross-section can be calculated based on Equation (5):[20]

$$\sigma(\lambda) = \frac{\lambda^4 E_F(\lambda)}{8\pi n^2(\lambda) c \tau_F} \quad (5)$$

where λ is the wavelength, $n(\lambda)$ is the refractive index, c is the vacuum light velocity, τ_F is the PL lifetime, and $E_F(\lambda)$ is the PL quantum distribution versus wavelength. The stimulated emission cross-section is proportional to the ratio of PL quantum yield to PL lifetime, that is, the radiative recombination rate. This indicates a ≈5000 fold increase in the stimulated emission cross-section for the Al_2O_3-modified $CsPbBr_3$ perovskite, which would significantly improve the optical gain of $CsPbBr_3$ perovskites.

The optical gain in $CsPbBr_3$ perovskite films with and without Al_2O_3 coating was investigated through optically pumped amplified spontaneous emission (ASE) (Figure S9).[21] The PL spectra of $CsPbBr_3$ perovskite films were collected under excitation with increasing energy fluence (Figure 6a,b). At low pump fluences, the $CsPbBr_3$ films exhibit broad PL spectra, corresponding to the spontaneous emission.[22] When the pump fluence exceeds certain thresholds, the PL from $CsPbBr_3$ films experiences a notable spectral narrowing and a dramatic intensity increase, indicating the occurrence of ASE.[23] The nonlinear response of the light emission intensity to pump fluence confirms the ASE behaviors in both kinds of $CsPbBr_3$ perovskite films (Figure 6c).[24] From the pump fluence-dependent PL intensities, we derived the ASE thresholds of 51.5 and 20.6 $\mu J\,cm^{-2}$ for the bare and Al_2O_3-modified $CsPbBr_3$ films, respectively. The notable reduction of ASE threshold in $CsPbBr_3$ perovskite films after Al_2O_3 coating is attributed to the increase in the stimulated emission cross-section. Besides improving its optical gain, the Al_2O_3 coating endows the $CsPbBr_3$ perovskite with high stability.[25] We recorded the ASE intensities of the $CsPbBr_3$ perovskite films under continuous excitation of 5 hours (Figure 6d). The ASE intensity from the bare $CsPbBr_3$ film starts to decline significantly after 2 hours and drops down to 46 % of its initial output intensity after 5 hours, while the Al_2O_3 encapsulated $CsPbBr_3$ film maintains 90 % of its initial ASE intensity after 5 hours. Overall, the Al_2O_3-coated $CsPbBr_3$ perovskite fully demonstrates stable and efficient optical gain.

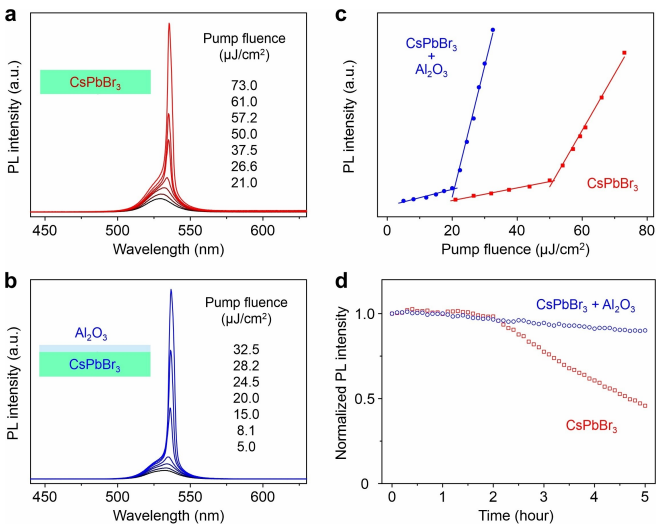

Figure 6. a,b) PL spectra of bare and Al_2O_3-coated $CsPbBr_3$ perovskite films under excitation with increasing energy fluence. c) PL intensities of the $CsPbBr_3$ perovskite films with and without Al_2O_3 coating as a function of pump fluence. d) Normalized ASE intensities of these $CsPbBr_3$ perovskite films under continuous operation of 5 hours at ambient conditions.

Conclusion

In summary, we realized a giant enhancement of the radiative recombination rate in metal halide perovskites with an interfacial chemistry strategy. The $CsPbBr_3$ perovskite film was chemically modified by Al_2O_3, producing a perovskite-oxide interfacial hybrid system. After the Al_2O_3 modification, the perovskite film exhibited a ≈500 fold PL enhancement and a ≈10 fold PL lifetime reduction, indicating an unprecedented ≈5000 fold increase in the radiative recombination rate. By exploring the excited-state dynamics and electronic band structures, the giant enhancement of radiative recombination was attributed to the formation of oxide-bonded perovskite surface states with a large exciton binding energy and a high localized density of electronic state. The enormously enhanced radiative recombination rate significantly improved the optical gain in the $CsPbBr_3$ perovskite film. Our experimental finding opens up an avenue to optimize metal halide perovskites with high performance for optoelectronic applications.

Acknowledgements

The authors thank R. Engelhard, C. Schmidt, S. Nestler and L. Raith for the technical support. This work was financially

supported by the Würzburg-Dresden Cluster of Excellence on Complexity and Topology in Quantum Matter-ct.qmat (EXC 2147, project-ID 390858490) and German Research Foundation (MA 7968/2-1). C.Z. acknowledges financial support from the National Natural Science Foundation of China (Grant No. 51903238). Y.S.Z. acknowledges financial support from the Ministry of Science and Technology of China (Grant No. 2017YFA0204502). O.G.S. acknowledges financial support by the Leibniz Program of the German Research Foundation (SCHM 1298/26-1). Open Access funding enabled and organized by Projekt DEAL.

Conflict of Interest

The authors declare no conflict of interest.

Data Availability Statement

The data that support the findings of this study are available from the corresponding author upon reasonable request.

Keywords: Amplified Spontaneous Emission · Interfacial Chemistry · Luminescence · Metal Halide Perovskite · Radiative Recombination

[1] a) W. Zhang, G. E. Eperon, H. J. Snaith, *Nat. Energy* **2016**, *1*, 16048; b) F. P. García de Arquer, A. Armin, P. Meredith, E. H. Sargent, *Nat. Rev. Mater.* **2017**, *2*, 16100; c) X. K. Liu, W. Xu, S. Bai, Y. Jin, J. Wang, R. H. Friend, F. Gao, *Nat. Mater.* **2021**, *20*, 10–21; d) H. Dong, C. Zhang, X. Liu, J. Yao, Y. S. Zhao, *Chem. Soc. Rev.* **2020**, *49*, 951–982; e) Q. Zhang, Q. Shang, R. Su, T. T. H. Do, Q. Xiong, *Nano Lett.* **2021**, *21*, 1903–1914.

[2] a) D. Luo, R. Su, W. Zhang, Q. Gong, R. Zhu, *Nat. Rev. Mater.* **2020**, *5*, 44–60; b) Y. H. Kim, H. Cho, T. W. Lee, *Proc. Natl. Acad. Sci. USA* **2016**, *113*, 11694–11702; c) Y. Jiang, X. Wang, A. Pan, *Adv. Mater.* **2019**, *31*, 1806671; d) S. D. Stranks, R. L. Z. Hoye, D. Di, R. H. Friend, F. Deschler, *Adv. Mater.* **2019**, *31*, 1803336; e) K. Wang, G. Xing, Q. Song, S. Xiao, *Adv. Mater.* **2021**, *33*, 2000306.

[3] a) H. Cho, S.-H. Jeong, M.-H. Park, Y.-H. Kim, C. Wolf, C.-L. Lee, J. H. Heo, A. Sadhanala, N. Myoung, S. Yoo, S. H. Im, R. H. Friend, T.-W. Lee, *Science* **2015**, *350*, 1222–1225; b) N. Wang, L. Cheng, R. Ge, S. Zhang, Y. Miao, W. Zou, C. Yi, Y. Sun, Y. Cao, R. Yang, Y. Wei, Q. Guo, Y. Ke, M. Yu, Y. Jin, Y. Liu, Q. Ding, D. Di, L. Yang, G. Xing, H. Tian, C. Jin, F. Gao, R. H. Friend, J. Wang, W. Huang, *Nat. Photonics* **2016**, *10*, 699; c) M. Yuan, L. N. Quan, R. Comin, G. Walters, R. Sabatini, O. Voznyy, S. Hoogland, Y. Zhao, E. M. Beauregard, P. Kanjanaboos, Z. Lu, D. H. Kim, E. H. Sargent, *Nat. Nanotechnol.* **2016**, *11*, 872–877; d) J. S. Yao, J. Ge, K. H. Wang, G. Zhang, B. S. Zhu, C. Chen, Q. Zhang, Y. Luo, S. H. Yu, H. B. Yao, *J. Am. Chem. Soc.* **2019**, *141*, 2069–2079; e) J. Shamsi, A. S. Urban, M. Imran, L. De Trizio, L. Manna, *Chem. Rev.* **2019**, *119*, 3296–3348; f) Y. Liang, Q. Shang, Q. Wei, L. Zhao, Z. Liu, J. Shi, Y. Zhong, J. Chen, Y. Gao, M. Li, X. Liu, G. Xing, Q. Zhang, *Adv. Mater.* **2019**, *31*, 1903030.

[4] a) J. Luo, X. Wang, S. Li, J. Liu, Y. Guo, G. Niu, L. Yao, Y. Fu, L. Gao, Q. Dong, C. Zhao, M. Leng, F. Ma, W. Liang, L. Wang, S. Jin, J. Han, L. Zhang, J. Etheridge, J. Wang, Y. Yan, E. H. Sargent, J. Tang, *Nature* **2018**, *563*, 541–545; b) J. S. Yao, J. Ge, B. N. Han, K. H. Wang, H. B. Yao, H. L. Yu, J. H. Li, B. S. Zhu, J. Z. Song, C. Chen, Q. Zhang, H. B. Zeng, Y. Luo, S. H. Yu, *J. Am. Chem. Soc.* **2018**, *140*, 3626–3634; c) S. Feldmann, S. Macpherson, S. P. Senanayak, M. Abdi-Jalebi, J. P. H. Rivett, G. Nan, G. D. Tainter, T. A. S. Doherty, K. Frohna, E. Ringe, R. H. Friend, H. Sirringhaus, M. Saliba, D. Beljonne, S. D. Stranks, F. Deschler, *Nat. Photonics* **2020**, *14*, 123–128; d) X. Shen, Y. Zhang, S. V. Kershaw, T. Li, C. Wang, X. Zhang, W. Wang, D. Li, Y. Wang, M. Lu, L. Zhang, C. Sun, D. Zhao, G. Qin, X. Bai, W. W. Yu, A. L. Rogach, *Nano Lett.* **2019**, *19*, 1552–1559.

[5] a) B. Gholipour, G. Adamo, D. Cortecchia, H. N. Krishnamoorthy, M. D. Birowosuto, N. I. Zheludev, C. Soci, *Adv. Mater.* **2017**, *29*, 1604268; b) S. V. Makarov, V. Milichko, E. V. Ushakova, M. Omelyanovich, A. Cerdan Pasaran, R. Haroldson, B. Balachandran, H. Wang, W. Hu, Y. S. Kivshar, A. A. Zakhidov, *ACS Photonics* **2017**, *4*, 728–735; c) G. Adamo, H. N. Swaha Krishnamoorthy, D. Cortecchia, B. Chaudhary, V. Nalla, N. I. Zheludev, C. Soci, *Nano Lett.* **2020**, *20*, 7906–7911.

[6] a) N. Pourdavoud, S. Wang, A. Mayer, T. Hu, Y. Chen, A. Marianovich, W. Kowalsky, R. Heiderhoff, H.-C. Scheer, T. Riedl, *Adv. Mater.* **2017**, *29*, 1605003; b) N. Pourdavoud, T. Haeger, A. Mayer, P. J. Cegielski, A. L. Giesecke, R. Heiderhoff, S. Olthof, S. Zaefferer, I. Shutsko, A. Henkel, D. Becker-Koch, M. Stein, M. Cehovski, O. Charfi, H. H. Johannes, D. Rogalla, M. C. Lemme, M. Koch, Y. Vaynzof, K. Meerholz, W. Kowalsky, H. C. Scheer, P. Gorrn, T. Riedl, *Adv. Mater.* **2019**, *31*, 1903717; c) Y. Liang, Q. Y. Shang, M. L. Li, S. Zhang, X. F. Liu, Q. Zhang, *Adv. Funct. Mater.* **2021**, *31*, 2106108.

[7] a) I. L. Braly, D. W. deQuilettes, L. M. Pazos-Outón, S. Burke, M. E. Ziffer, D. S. Ginger, H. W. Hillhouse, *Nat. Photonics* **2018**, *12*, 355–361; b) Q. Jiang, Y. Zhao, X. Zhang, X. Yang, Y. Chen, Z. Chu, Q. Ye, X. Li, Z. Yin, J. You, *Nat. Photonics* **2019**, *13*, 460–466; c) H. Ren, S. D. Yu, L. F. Chao, Y. D. Xia, Y. H. Sun, S. W. Zuo, F. Li, T. T. Niu, Y. G. Yang, H. X. Ju, B. X. Li, H. Y. Du, X. Y. Gao, J. Zhang, J. P. Wang, L. J. Zhang, Y. H. Chen, W. Huang, *Nat. Photonics* **2020**, *14*, 154–163; d) D. P. Nenon, K. Pressler, J. Kang, B. A. Koscher, J. H. Olshansky, W. T. Osowiecki, M. A. Koc, L. W. Wang, A. P. Alivisatos, *J. Am. Chem. Soc.* **2018**, *140*, 17760–17772; e) J. Tong, Z. Song, D. H. Kim, X. Chen, C. Chen, A. F. Palmstrom, P. F. Ndione, M. O. Reese, S. P. Dunfield, O. G. Reid, J. Liu, F. Zhang, S. P. Harvey, Z. Li, S. T. Christensen, G. Teeter, D. Zhao, M. M. Al-Jassim, M. F. A. M. van Hest, M. C. Beard, S. E. Shaheen, J. J. Berry, Y. Yan, K. Zhu, *Science* **2019**, *364*, 475–479; f) B. J. Bohn, Y. Tong, M. Gramlich, M. L. Lai, M. Doblinger, K. Wang, R. L. Z. Hoye, P. Muller-Buschbaum, S. D. Stranks, A. S. Urban, L. Polavarapu, J. Feldmann, *Nano Lett.* **2018**, *18*, 5231–5238; g) J. Ye, M. M. Byranvand, C. O. Martínez, R. L. Z. Hoye, M. Saliba, L. Polavarapu, *Angew. Chem. Int. Ed.* **2021**, *60*, 21636–21660; *Angew. Chem.* **2021**, *133*, 21804–21828.

[8] S. Feldmann, M. K. Gangishetty, I. Bravic, T. Neumann, B. Peng, T. Winkler, R. H. Friend, B. Monserrat, D. N. Congreve, F. Deschler, *J. Am. Chem. Soc.* **2021**, *143*, 8647–8653.

[9] Y. Fu, H. Zhu, C. C. Stoumpos, Q. Ding, J. Wang, M. G. Kanatzidis, X. Zhu, S. Jin, *ACS Nano* **2016**, *10*, 7963–7972.

[10] D. Lu, Y. Zhang, M. Lai, A. Lee, C. Xie, J. Lin, T. Lei, Z. Lin, C. S. Kley, J. Huang, E. Rabani, P. Yang, *Nano Lett.* **2018**, *18*, 6967–6973.

[11] Q. Xiang, B. Zhou, K. Cao, Y. Wen, Y. Li, Z. Wang, C. Jiang, B. Shan, R. Chen, *Chem. Mater.* **2018**, *30*, 8486–8494.

[12] a) Y. Tong, E. Bladt, M. F. Aygüler, A. Manzi, K. Z. Milowska, V. A. Hintermayr, P. Docampo, S. Bals, A. S. Urban, L. Polavarapu, J. Feldmann, *Angew. Chem. Int. Ed.* **2016**, *55*, 13887–13892; *Angew. Chem.* **2016**, *128*, 14091–14096; b) H.

Zhou, S. Yuan, X. Wang, T. Xu, X. Wang, H. Li, W. Zheng, P. Fan, Y. Li, L. Sun, A. Pan, *ACS Nano* **2017**, *11*, 1189–1195; c) X. Wang, M. Shoaib, X. Wang, X. Zhang, M. He, Z. Luo, W. Zheng, H. Li, T. Yang, X. Zhu, L. Ma, A. Pan, *ACS Nano* **2018**, *12*, 6170–6178; d) A. Dey, J. Ye, A. De, E. Debroye, S. K. Ha, E. Bladt, A. S. Kshirsagar, Z. Wang, J. Yin, Y. Wang, L. N. Quan, F. Yan, M. Gao, X. Li, J. Shamsi, T. Debnath, M. Cao, M. A. Scheel, S. Kumar, J. A. Steele, M. Gerhard, L. Chouhan, K. Xu, X. G. Wu, Y. Li, Y. Zhang, A. Dutta, C. Han, I. Vincon, A. L. Rogach, A. Nag, A. Samanta, B. A. Korgel, C. J. Shih, D. R. Gamelin, D. H. Son, H. Zeng, H. Zhong, H. Sun, H. V. Demir, I. G. Scheblykin, I. Mora-Sero, J. K. Stolarczyk, J. Z. Zhang, J. Feldmann, J. Hofkens, J. M. Luther, J. Perez-Prieto, L. Li, L. Manna, M. I. Bodnarchuk, M. V. Kovalenko, M. B. J. Roeffaers, N. Pradhan, O. F. Mohammed, O. M. Bakr, P. Yang, P. Muller-Buschbaum, P. V. Kamat, Q. Bao, Q. Zhang, R. Krahne, R. E. Galian, S. D. Stranks, S. Bals, V. Biju, W. A. Tisdale, Y. Yan, R. L. Z. Hoye, L. Polavarapu, *ACS Nano* **2021**, *15*, 10775–10981.

[13] a) K. Wei, Z. Xu, R. Chen, X. Zheng, X. Cheng, T. Jiang, *Opt. Lett.* **2016**, *41*, 3821–3824; b) A. D. Wright, C. Verdi, R. L. Milot, G. E. Eperon, M. A. Pérez-Osorio, H. J. Snaith, F. Giustino, M. B. Johnston, L. M. Herz, *Nat. Commun.* **2016**, *7*, 11755; c) H. Zhou, J. Park, Y. Lee, J. M. Park, J. H. Kim, J. S. Kim, H. D. Lee, S. H. Jo, X. Cai, L. Li, X. Sheng, H. J. Yun, J. W. Park, J. Y. Sun, T. W. Lee, *Adv. Mater.* **2020**, *32*, 2001989.

[14] a) M. Rodová, J. Brožek, K. Knížek, K. Nitsch, *J. Therm. Anal. Calorim.* **2003**, *71*, 667–673; b) D. C. Miller, R. R. Foster, S.-H. Jen, J. A. Bertrand, S. J. Cunningham, A. S. Morris, Y.-C. Lee, S. M. George, M. L. Dunn, *Sens. Actuators A* **2010**, *164*, 58–67.

[15] D. A. Egger, A. Bera, D. Cahen, G. Hodes, T. Kirchartz, L. Kronik, R. Lovrincic, A. M. Rappe, D. R. Reichman, O. Yaffe, *Adv. Mater.* **2018**, *30*, 1800691.

[16] a) M. D. Smith, B. A. Connor, H. I. Karunadasa, *Chem. Rev.* **2019**, *119*, 3104–3139; b) J. Hou, Z. Wang, P. Chen, V. Chen, A. K. Cheetham, L. Wang, *Angew. Chem. Int. Ed.* **2020**, *59*, 19434–19449; *Angew. Chem.* **2020**, *132*, 19602–19617.

[17] a) H. Zhu, M. T. Trinh, J. Wang, Y. Fu, P. P. Joshi, K. Miyata, S. Jin, X. Y. Zhu, *Adv. Mater.* **2017**, *29*, 1603072; b) N. Droseros, G. Longo, J. C. Brauer, M. Sessolo, H. J. Bolink, N. Banerji, *ACS Energy Lett.* **2018**, *3*, 1458–1466.

[18] a) G. R. Yettapu, D. Talukdar, S. Sarkar, A. Swarnkar, A. Nag, P. Ghosh, P. Mandal, *Nano Lett.* **2016**, *16*, 4838–4848; b) J. Song, Q. Cui, J. Li, J. Xu, Y. Wang, L. Xu, J. Xue, Y. Dong, T. Tian, H. Sun, H. Zeng, *Adv. Opt. Mater.* **2017**, *5*, 1700157.

[19] a) G. Kresse, J. Hafner, *Phys. Rev. B* **1993**, *47*, 558–561; b) G. Kresse, J. Furthmüller, *Comput. Mater. Sci.* **1996**, *6*, 15–50; c) G. Kresse, J. Furthmüller, *Phys. Rev. B* **1996**, *54*, 11169–11186; d) J. P. Perdew, K. Burke, M. Ernzerhof, *Phys. Rev. Lett.* **1996**, *77*, 3865–3868; e) P. E. Blöchl, *Phys. Rev. B* **1994**, *50*, 17953–17979; f) G. Kresse, D. Joubert, *Phys. Rev. B* **1999**, *59*, 1758–1775; g) S. Grimme, J. Antony, S. Ehrlich, H. Krieg, *J. Chem. Phys.* **2010**, *132*, 154104; h) H. J. Monkhorst, J. D. Pack, *Phys. Rev. B* **1976**, *13*, 5188–5192.

[20] H. Dong, C. Zhang, X. Lin, Z. Zhou, J. Yao, Y. S. Zhao, *Nano Lett.* **2017**, *17*, 91–96.

[21] H. Dong, C. N. Saggau, M. Zhu, J. Liang, S. Duan, X. Wang, H. Tang, Y. Yin, X. Wang, J. Wang, C. Zhang, Y. S. Zhao, L. Ma, O. G. Schmidt, *Adv. Funct. Mater.* **2021**, *31*, 2109080.

[22] X. Wang, H. Zhou, S. Yuan, W. Zheng, Y. Jiang, X. Zhuang, H. Liu, Q. Zhang, X. Zhu, X. Wang, A. Pan, *Nano Res.* **2017**, *10*, 3385–3395.

[23] a) G. Xing, N. Mathews, S. S. Lim, N. Yantara, X. Liu, D. Sabba, M. Gratzel, S. Mhaisalkar, T. C. Sum, *Nat. Mater.* **2014**, *13*, 476–480; b) Y. Wang, X. Li, J. Song, L. Xiao, H. Zeng, H. Sun, *Adv. Mater.* **2015**, *27*, 7101–7108; c) Y. Jia, R. A. Kerner, A. J. Grede, B. P. Rand, N. C. Giebink, *Nat. Photonics* **2017**, *11*, 784–788.

[24] a) H. Zhang, Y. Wu, Q. Liao, Z. Zhang, Y. Liu, Q. Gao, P. Liu, M. Li, J. Yao, H. Fu, *Angew. Chem. Int. Ed.* **2018**, *57*, 7748–7752; *Angew. Chem.* **2018**, *130*, 7874–7878; b) C. Qin, A. S. D. Sandanayaka, C. Zhao, T. Matsushima, D. Zhang, T. Fujihara, C. Adachi, *Nature* **2020**, *585*, 53–57.

[25] a) Z. Li, L. Kong, S. Huang, L. Li, *Angew. Chem. Int. Ed.* **2017**, *56*, 8134–8138; *Angew. Chem.* **2017**, *129*, 8246–8250; b) A. Loiudice, S. Saris, E. Oveisi, D. T. L. Alexander, R. Buonsanti, *Angew. Chem. Int. Ed.* **2017**, *56*, 10696–10701; *Angew. Chem.* **2017**, *129*, 10836–10841; c) H. Yu, X. Xu, H. Liu, Y. Wan, X. Cheng, J. Chen, Y. Ye, L. Dai, *ACS Nano* **2020**, *14*, 552–558; d) Y. Y. Duan, D. Y. Wang, R. D. Costa, *Adv. Funct. Mater.* **2021**, *31*, 2104634.

Manuscript received: November 22, 2021
Accepted manuscript online: January 23, 2022
Version of record online: February 7, 2022